

EXPERIENCE WITH THE KFA/IGV (JUELICH) MAGNETIC BEARING SYSTEM ON AN SNS
NEUTRON CHOPPER

T J L Jones, J H Parker and I Davidson
Rutherford Appleton Laboratory

K Boden and J K Fremery
IGV, KFA Jülich

1. Introduction

The chopper described is the fast Fermi neutron beam chopper which has been designed to select the incident neutron energy for the High Energy Transfer Spectrometer (HET) on the SNS, the magnetic suspension system for which has been developed and manufactured as the result of a collaborative contract between the Rutherford Appleton Laboratory (RAL) and the Institut für Grenzflächenforschung und Vakuumphysik at Kernforschungsanlage Jülich (KFA/IGV).

Figure 1 shows a sectional assembly drawing of the chopper. It consists essentially of 4 major components:

- i) An evacuable spinning tank.
- ii) The chopper rotor.
- iii) The upper magnetic bearing assembly.
- iv) The lower magnetic bearing assembly to which is attached the stator assembly of the hysteresis motor which drives the chopper rotor.

Figure 2 is a photograph of the chopper assembly with the top cover of the vacuum tank and upper bearing assembly raised to show the top end of the chopper rotor.

2. The Construction of the rotor and slit packages

The chopper is furnished with a family of 3 rotors containing curved-slot slit packages. These are assemblies of neutron opaque 'slats', formed from a triple laminate of boron fibres diffusion bonded into an aluminium matrix, interleaved with neutron transmitting 'slits' built up from appropriate thicknesses of etched aluminium foil. Cylindrically profiled cheek plates are used to curve the packages so that, at the rotor speed of 600 Hz, their transmissions and resolution are optimised to neutron energies of 1 eV, 500 meV and 250 meV respectively.

Because the magnetic bearings operate with a large physical clearance between rotor and stator the rotors are easily interchanged in the spinning tank and so, by choice of appropriate rotor and electronic rephasing of the chopper, incident neutrons with energies ranging from ~ 100 meV to almost 4 eV can be selected for the spectrometer at $\sim 1\%$ energy resolution.

The construction of a rotor can be clearly seen in Figure 3 which is a photograph taken just before the insertion of a slit package into the central body of the rotor. To the left of the slit package examples of the component 'slats' and etched 'slits' are shown and the rods, which fit into the reamed grooves in the package securing it centrally in the rotor body, can be seen protruding from the upper side. (The plates which can be seen screwed to the ends of the package are only mounting jigs to hold the assembly together during manufacture and are removed after the package has been press-fitted into the body.) The upper and lower shafts, to the left and right of the central body in the photograph, which are integral with the aluminium rotor body, are fitted with steel collars which are the moving components of the magnetic bearing and hysteresis motor systems. At the extremities of these shafts dry-lubricated ball races are fitted which act as touch-down and safety bearings in the event of failure of the magnetic suspension.

3. The Magnetic Bearing and Control System

Frictionless suspension of the rotors is achieved using an axially-passive, radially-active permanent magnet bearing system developed by KFA/IGV.

Magnetic bearing stator units are mounted on the upper and lower flanges of the spinning tank. The passive part of each unit is a toroidal barium-ferrite permanent magnet which provides the force to support the weight of the rotor and much of the force to centre it. The active part of each stator consists of two pairs of horizontally opposed magnetoresistors, which sense the off-axis deviations of the rotating steel collars attached to the rotor, and two pairs of horizontally opposed force coils which are powered by the electronic servo control to provide the restoring forces needed to re-centre the rotor.

The drive stator of the hysteresis motor is attached to the outer end of the lower bearing stator. The stator assemblies are sleeved internally with, 'O' ring sealed, thin stainless steel liners which isolates all components from the vacuum within the spinning tank.

The only bearing components attached to the rotors are a set of mild steel cylindrical collars which are push-fitted and clamped to the upper and lower shafts. The motor drive collar is made of a special hysteresis material which is encapsulated in a titanium shield.

A schematic circuit illustrating the principal of operation of the bearing and its control unit is shown in Figure 4. Outputs are also provided on the control unit which allow the magnitude and phase of the axial deviations of the upper and lower bearings to be monitored on an oscilloscope. Any changes in the dynamic balance of the rotor resulting from distortion or movement of the slit package due to the spinning forces are easily detected by this monitor.

4. Drive and Phasing Control Electronics

The chopper drive motor is of the hysteresis type with 3 phases. The stator is connected in a 4 wire 'star' configuration. At 120 Volts a:c line to starpoint it draws 1.2 Amps/phase and is capable of accelerating the chopper to its operational speed of 36000 rpm in ~ 20 minutes. After the chopper drops into phase at 600 Hz the motor current reduces to ≈ 0.6 Amps in order to protect the stator from overheating.

The motor is powered and controlled by a digital electronic control and drive system developed at RAL. The phase can be set in steps of $1.67 \mu\text{s}$ and under fixed frequency operation a phase stability of $\pm 0.2 \mu\text{s}$ has been achieved.

The drive and control system was fully described in a paper by T J L Jones and J H Parker presented at the ICANS IV Meeting.

5. First Results from Operation of the Chopper System

i) General conclusions on the magnetic bearing chopper

Because of the sealed modular construction of the magnetic bearing and motor stator units the chopper has been extremely easy to manufacture, install and operate. Interchange of the rotors has proved to be an easy task which can be performed in ~ 1 hr by the operational scientific staff, without the aid of fitters or mechanics.

ii) Results from operation in the test laboratory

Before installation on the HET Spectrometer the chopper was tested in the laboratory. All 3 rotors were spun at 600 Hz for periods of several days. Operation was silent and vibrationless and in all 3 cases the axial and phase stability of the rotors were within design specification. From observations of the monitor signals from the operating bearings and from visual examinations of the rotor packages after spinning, there were no indications of distortion or displacement of package components due to the action of the spinning forces.

iii) Neutronic performance of the chopper

Because the SNS only came into operation 1 week before this conference a full appraisal of the neutronic performance of the chopper has not yet been possible. To date only the 500 meV peak rotor has been used to monochromate neutrons to the HET Spectrometer.

In a series of short experiments the phase of the rotor was altered, with respect to the SNS neutron pulse, to sweep the neutron peak energy transmitted by the chopper from 310 meV to ~ 1 eV. A low efficiency scintillation detector, ~ 1.5 m in front of the chopper, was used to monitor the intensity of the incident neutron beam and observations were made of the signals from 2 monitor detectors situated in the direct beam 20 cm and ~ 7 m beyond the chopper and of simultaneous signals from the HET detector banks observing the scattered neutrons from a sample of ZrH₂ at the instrument sample position.

Due to interference from the stray magnetic fields (~ 20 Oersted) from the magnetic bearings the data from the monitor 20 cm beyond the chopper has proved non-valid. From the other data we make the following conclusions:

c) Neutron Pulse Characteristics

The duration of the neutron pulse transmitted by the chopper is $2 \mu\text{s}$ (FWHM) entirely consistent with the design of the 500 meV slit package. There is also transmission by the chopper $\sim 833 \mu\text{s}$ before the main pulse. This corresponds to $\frac{1}{2}$ revolution (π phase) of the chopper and, when the chopper is phased for 500 meV neutrons, represents transmission of neutrons with energies of $\sim 17 \text{ eV}$. A full investigation of this will be undertaken but the most probable explanation is that the tips of the slats are not completely neutron opaque at these energies and allow a direct line of sight through the rotor.

b) Relative Transmission of the Rotor

From these provisional data we have attempted to obtain the transmission of the rotor as a function of its opening time (t_{ch}) relative to the SNS pulse (transmitted peak neutron energy). This is shown in Figure 5. The results, which have been normalised for detector efficiency, whilst not entirely self consistent, show a peak transmission near the design energy of the rotor (500 meV). However the shape of the transmission curve is not in agreement with that predicted and further experiments are proceeding to resolve these differences.

6. Acknowledgements

The authors extend their thanks to all colleagues at the RAL and KFA laboratories who have aided with the design, installation and testing of this chopper, especially to Mr M Fisher, Dr A D Taylor and Mr W Rubner.

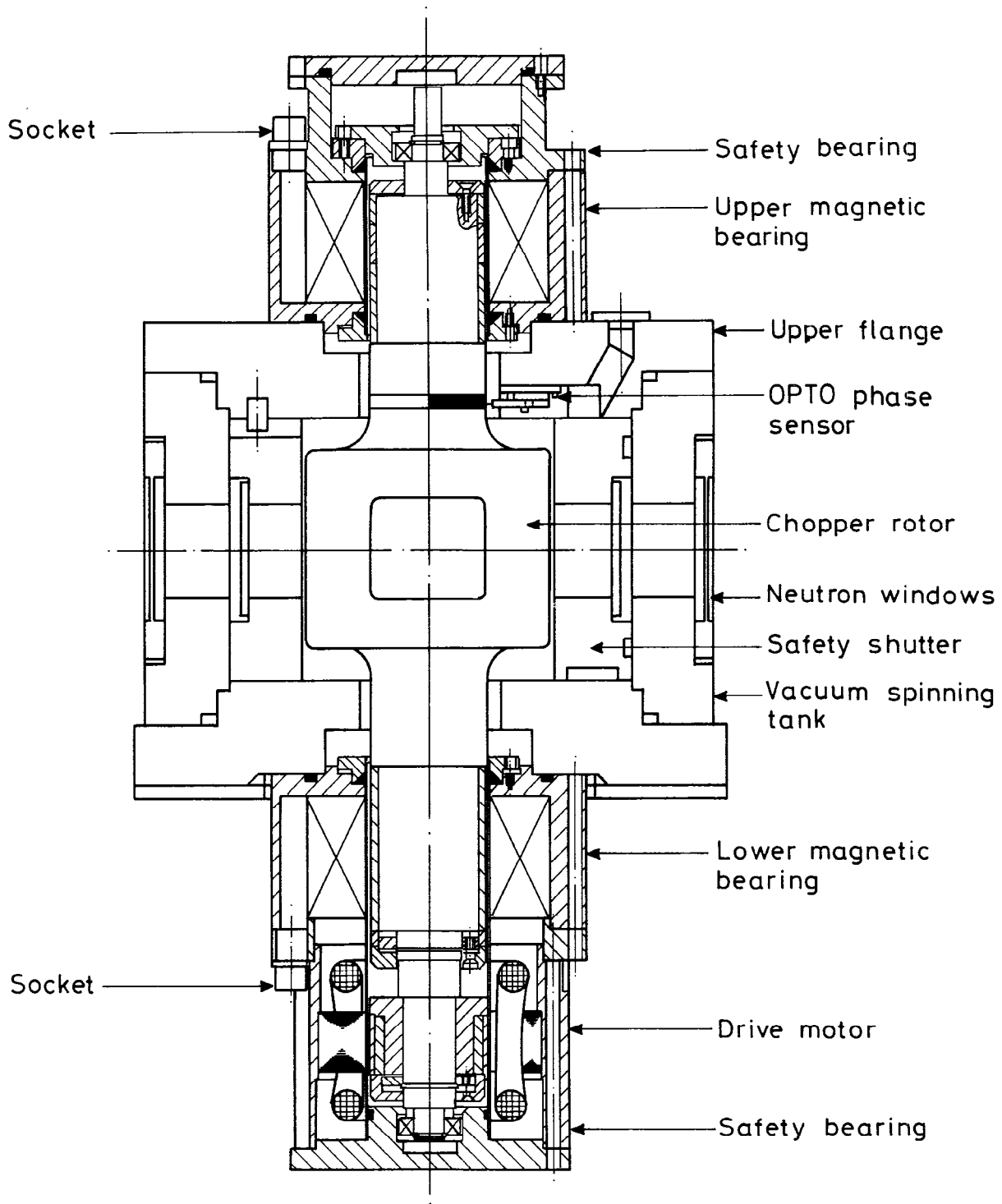


Figure 1 Sectional Assembly Drawing of the HET magnetically suspended chopper.

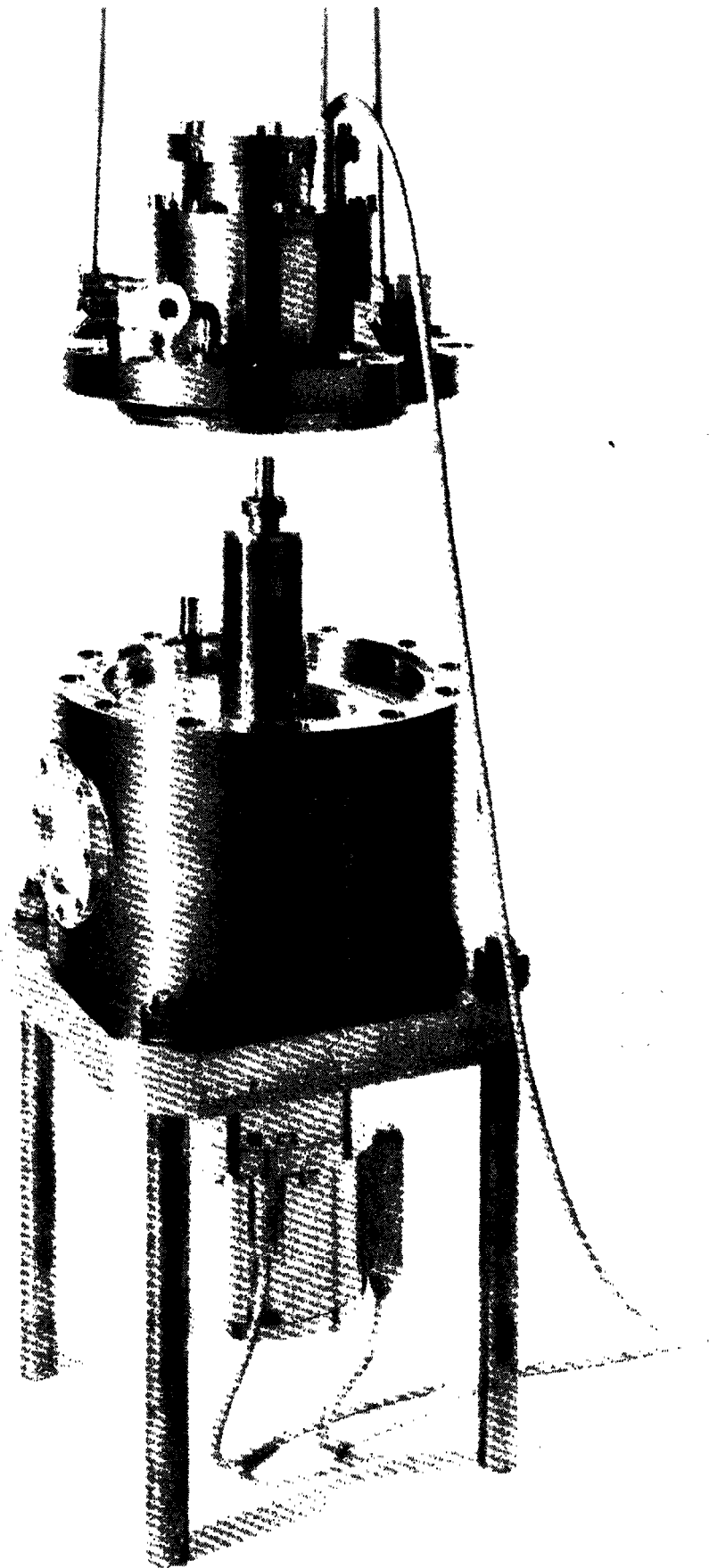


Figure 2 The chopper assembly with the upper bearing assembly and vacuum flange raised to show the mounted rotor.

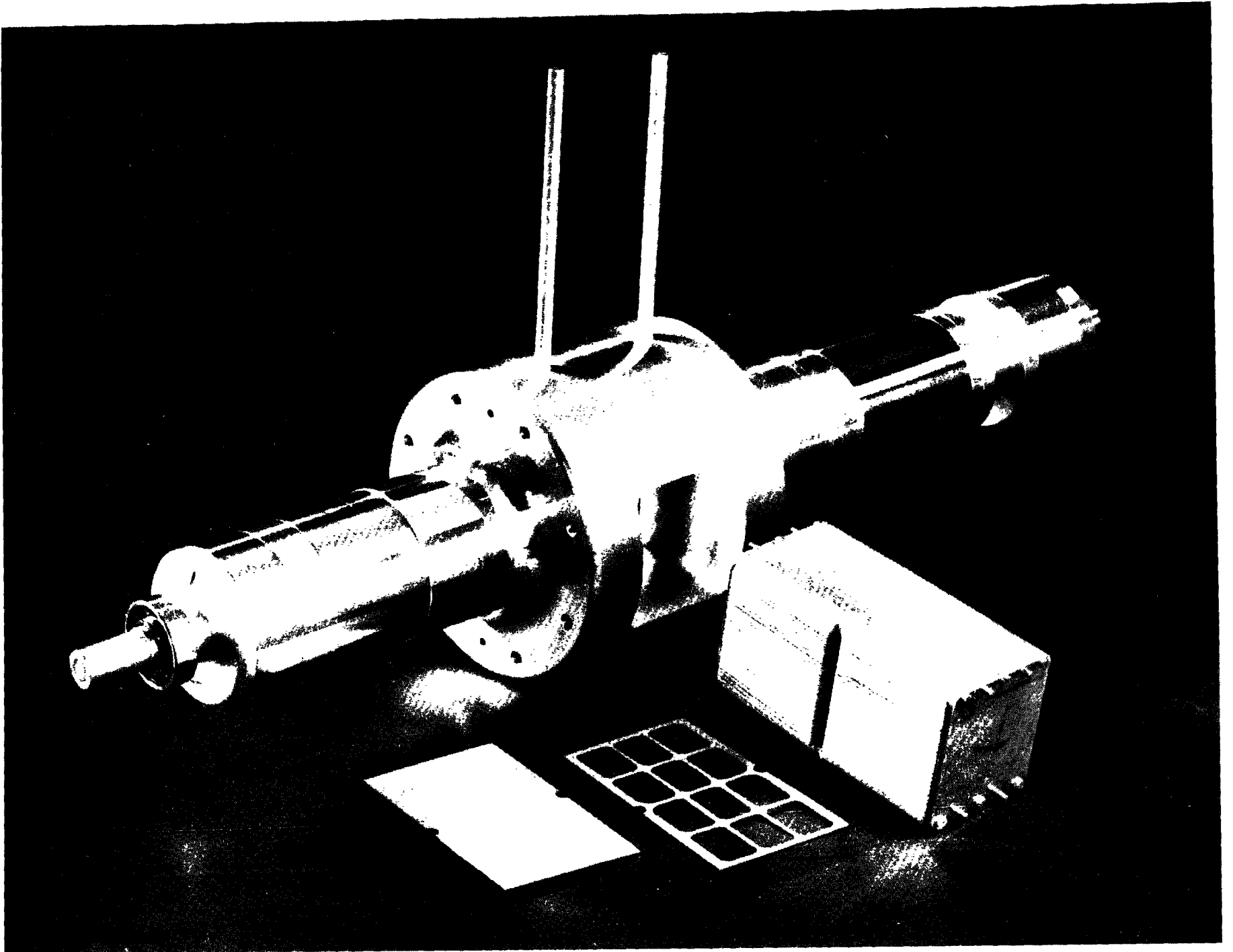


Figure 3 Construction of the chopper rotor and slit package.

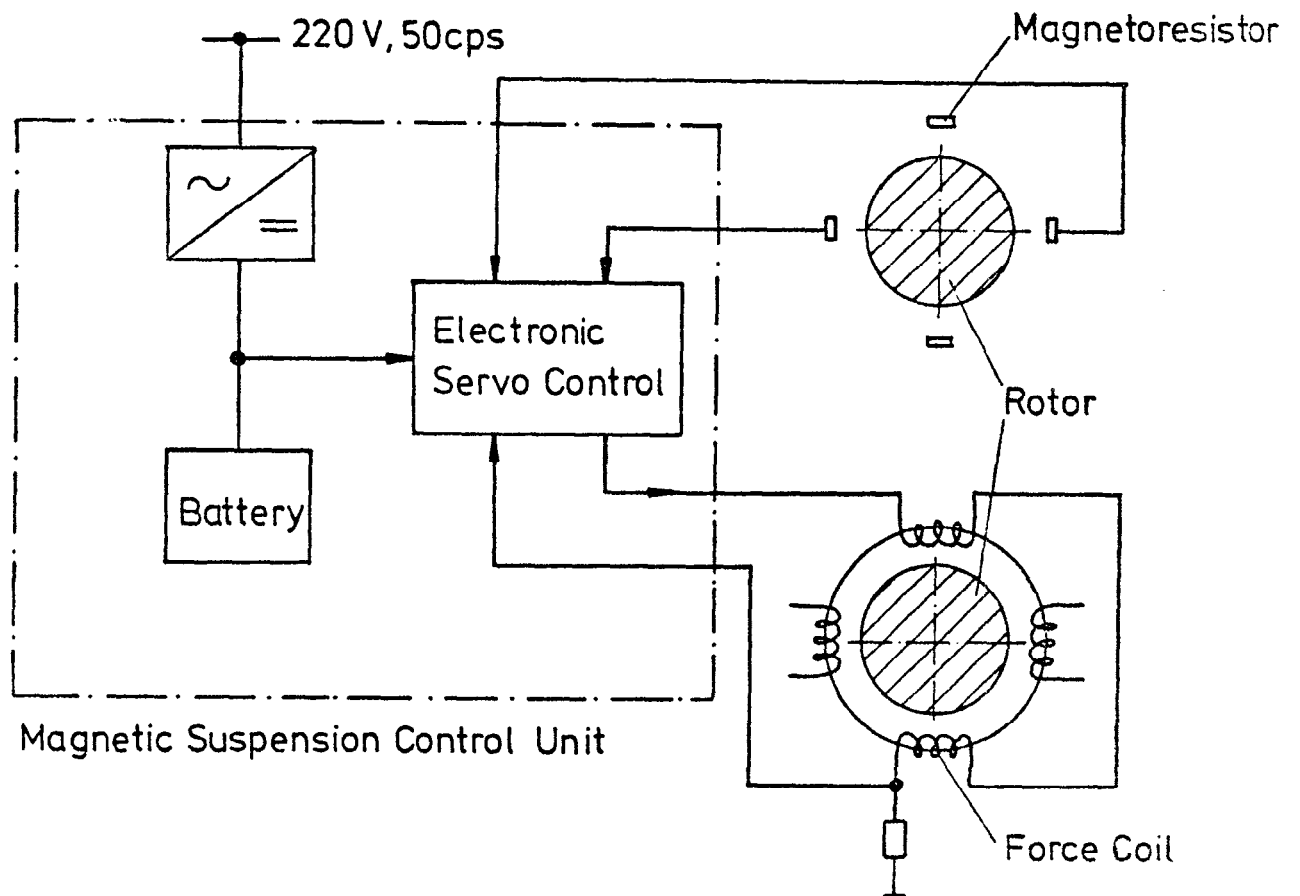


Figure 4 Schematic diagram of the magnetic bearing and its control circuit.

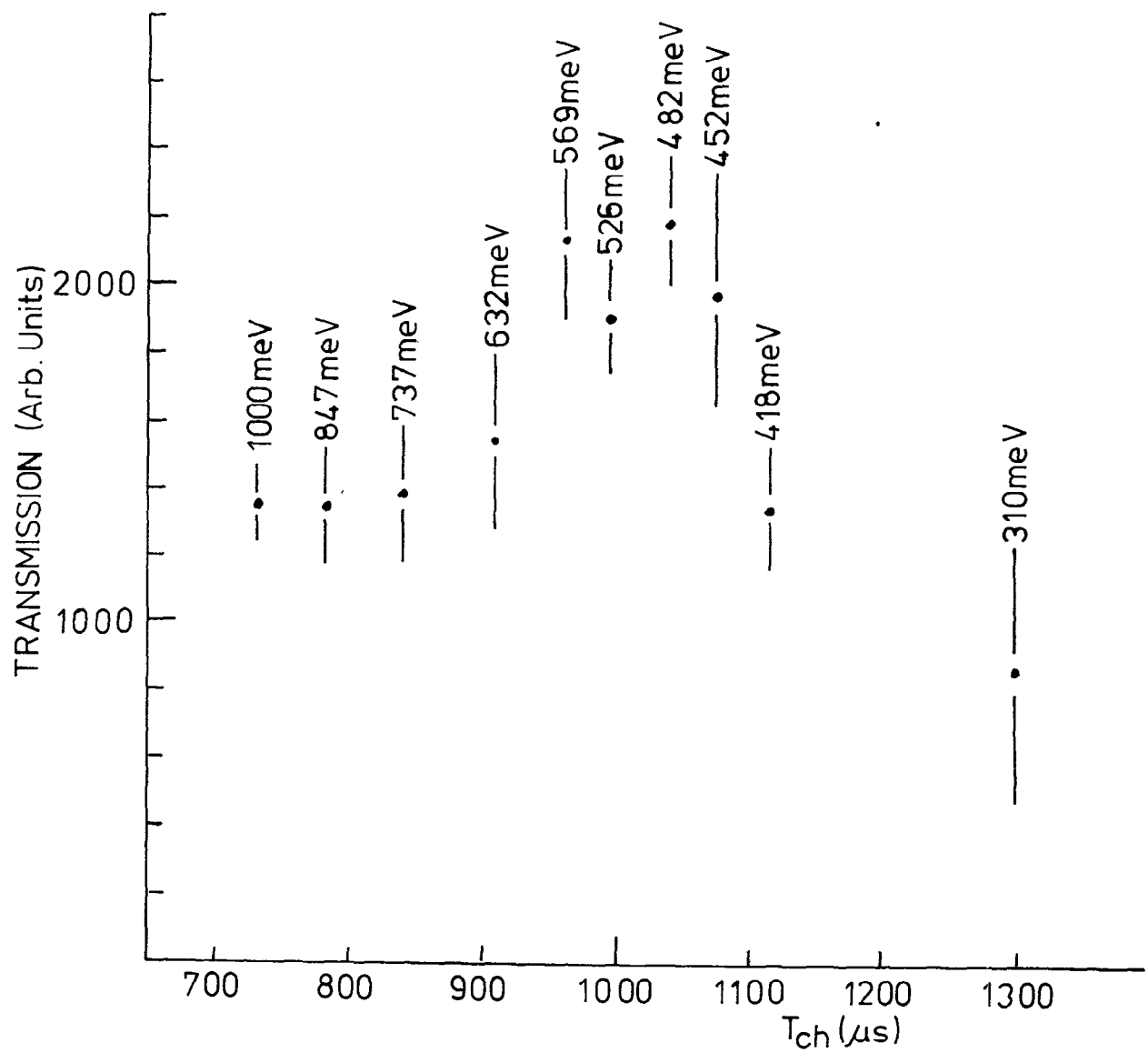


Figure 5 Provisional data for the relative transmission of the 500 meV chopper rotor.